

# Decoding the Pulse of Reasoning VLMs in Multi-Image Understanding Tasks

Chenjun Li

School of Electrical and Computer Engineering  
Cornell University  
c12733@cornell.edu

## Abstract

**Note:** *This is an on-going project. Results and methods are subject to change as experiments continue.*

Multi-image reasoning remains a significant challenge for vision-language models (VLMs). We investigate a previously overlooked phenomenon: during chain-of-thought (CoT) generation, the text-to-image (T2I) attention of reasoning VLMs exhibits diffuse “pulses”: sporadic and unfocused attention patterns that fail to concentrate on task-relevant images. We further reveal a systematic positional bias in attention allocation across images. Motivated by these observations, we propose PULSEFOCUS, a training-free, inference-time method that structures CoT reasoning into interleaved `<plan>/<focus:I>` blocks with soft attention gating. By forcing the model to explicitly plan which image to examine and then gating decode-time attention to the referenced image, PULSEFOCUS sharpens attention focus and yields consistent improvements on multi-image benchmarks like BLINK benchmark (+3.7%) and MuirBench (+1.07%).

## 1 Introduction

Recent vision-language models (VLMs) with reasoning capabilities, such as InternVL3.5 [15], Qwen3-VL [1], and GPT-5 [13], have demonstrated impressive single-image understanding. However, multi-image reasoning tasks requiring comparing, counting, ordering, or grounding across multiple images, remains substantially harder [14, 4, 6]. A growing number of benchmarks [14, 4, 11, 10] has exposed persistent failure modes: VLMs often confuse image identities, exhibit positional bias toward earlier images, and produce hallucinated cross-image comparisons [3].

We ask: *why* do VLMs struggle with multi-image tasks? Rather than attributing failure solely to insufficient training data or model capacity, we investigate the *internal attention dynamics* during chain-of-thought reasoning. Our analysis reveals two key phenomena:

1. **Diffuse T2I attention pulses.** During CoT generation, the model’s text-to-image (T2I) attention “pulses” sporadically across all images instead of concentrating on the image currently being discussed (Figure 1). This scattered attention correlates with reasoning errors.
2. **Positional attention bias.** Aggregating attention over many samples reveals systematic bias: earlier images receive more attention regardless of task relevance (Section 3).

These findings motivate PULSEFOCUS, a training-free inference-time intervention. PULSEFOCUS restructures CoT generation into explicit `<plan>/<focus:I>` blocks, where the model first plans which image(s) to examine, then generates observations with *soft attention gating* that amplifies attention to the referenced image while suppressing (but not eliminating) attention to others. This interleaved structure provides two benefits: (1) it forces systematic, image-by-image reasoning instead of ad-hoc jumps between images, and (2) the soft gating sharpens attention focus during each observation, reducing cross-image confusion.

We evaluate PULSEFOCUS across three multi-image benchmarks—MuirBench [14], BLINK [4], and Visual Haystacks [16]—using InternVL3.5 and Qwen3-VL model families. Our results show that PULSEFOCUS yields notable improvement on BLINK (+3.7% with phase-budget control) and competitive performance on

### Case 342: Counting with image identity confusion

Q: <image> <image> <image> <image> <image> <image> how many cars do you see in the given images?  
 Choices: (A) one | (B) two | (C) three | (D) None of the choices provided | GT: (B)



```

Baseline | Pred: (C) [wrong]
Token-level reasoning highlight: centered on I5
>all the images that contain cars. Then, I will count the number of
cars in those images to determine the correct answer choice.
Next focus: I3</plan>
<focus:I5>There is one car visible on the road in this image.</focus>
>
  
```

```

PulseFocus | Pred: (B) [correct]
Token-level reasoning highlight: centered on I5
>There is no car visible in this image.</focus>
<plan>Now, I'll check the fifth image.</plan>
<focus:I5>[There are two cars visible in this image, one white and
one dark-colored.</focus>
<plan>Finally, I'll look at the sixth image.</plan> ...
  
```

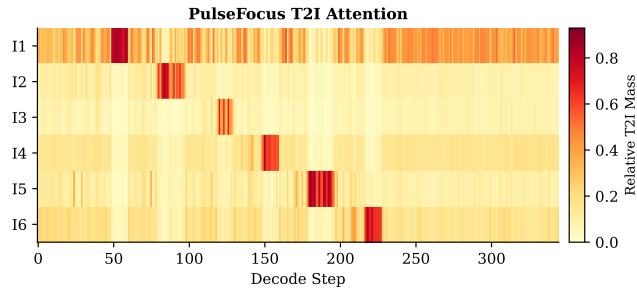
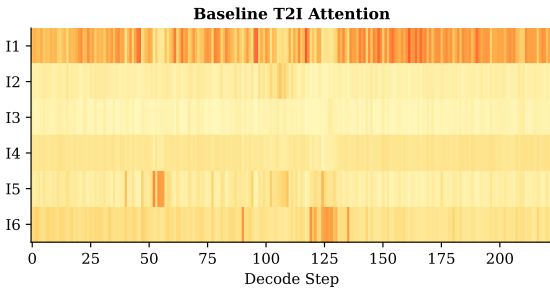


Figure 1: **Example case (from MuirBench).** Baseline CoT fails to focus on the key evidence image (I5): token-level T2I colouring remains diffuse, and the model cannot recognize the second car. With PULSEFOCUS, the <focus:I5> block becomes consistently image-aligned and the final answer is corrected from (C) to (B).

MuirBench, with qualitative analysis confirming sharper attention focus on case studies involving counting and image identity confusion.

## 2 Related Work

**Multi-Image VLMs and Benchmarks.** Multi-image understanding has been formalized through benchmarks including MuirBench [14] (12 reasoning capabilities over 2,600 samples), BLINK [4] (14 perceptual subtasks), MMIU [11], MIBench [10], and MMSI-Bench [18]. Model architectures such as InternVL3.5 [15] and Qwen3-VL [1] employ interleaved image-text representations with rotary position encoding, while training pipelines like Mantis [6] and LLaVA-OneVision [8] use curated multi-image instruction data.

**Failure Modes in Multi-Image Reasoning.** Wei et al. [3] identify systematic failure modes including image identity confusion and positional bias. Fan et al. [3] demonstrate that VLMs exhibit position-dependent performance degradation as image count increases. These studies diagnose the problem but do not intervene in the model’s internal attention mechanisms.

**Attention-Based Interventions.** Rethinking causal masking for VLMs [12] proposes non-causal attention across image tokens, while multi-layer learnable attention masks [2] train additional mask parameters. V2PE [5] introduces variable position encoding for better long-context multi-image handling. Unlike these approaches, PULSEFOCUS requires no training and operates purely at inference time through structured prompting and soft attention gating.

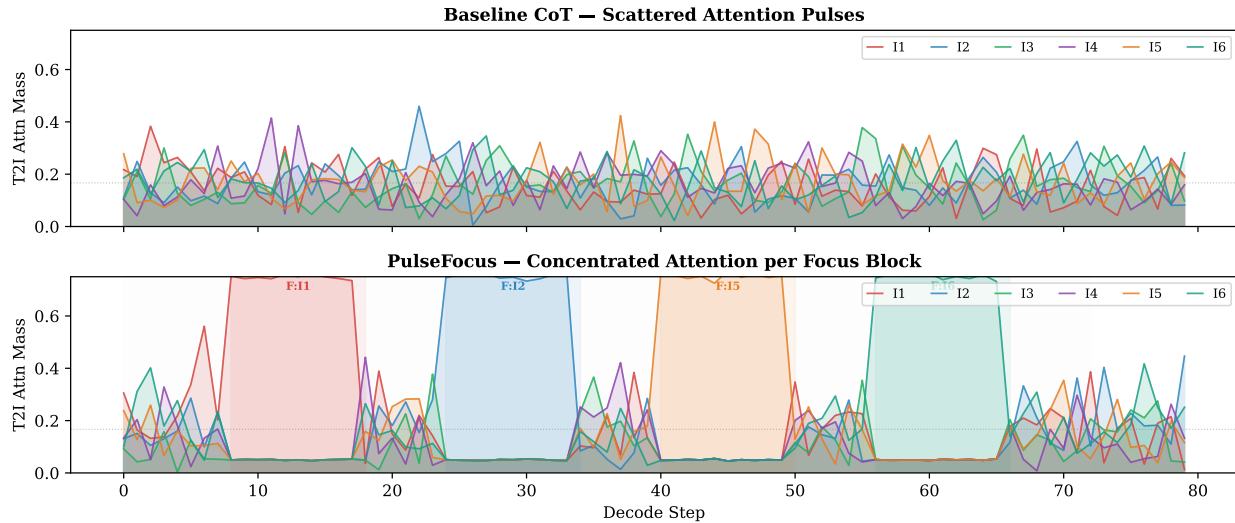


Figure 2: **Attention pulse visualization.** T2I attention mass per image over CoT decode steps for a counting task (the same example as in Figure 1, with six input images). Top: baseline—attention is spread across images even when discussing a specific image. Bottom: with PULSEFOCUS—attention concentrates on the image specified in the `<focus:I>` block. Colors indicate different images.

**Divide-and-Conquer Reasoning.** IdealGPT [19] decomposes VQA into iterative sub-questions, while divide-and-conquer approaches [9, 7] split complex reasoning into manageable steps. Interleaved reasoning via RL [17] shows that structured multi-hop reasoning improves over monolithic CoT. CMMCoT [20] augments CoT with memory for multi-image tasks. PULSEFOCUS shares the spirit of structured reasoning but uniquely combines it with attention-level gating to enforce focus.

### 3 Attention Analysis of Reasoning VLMs

We begin by analyzing the internal attention patterns of VLMs during multi-image CoT generation. All experiments in this section use InternVL3.5-8B on MuirBench [14].

#### 3.1 Text-to-Image Attention Pulses

During autoregressive CoT generation, we extract text-to-image attention weights at each decode step. For a generated token  $t_k$ , we compute the attention mass allocated to each image  $I_j$ :

$$a_{k,j} = \sum_{p \in \mathcal{S}_j} \alpha_{k,p} \quad (1)$$

where  $\mathcal{S}_j$  is the set of visual token positions for image  $I_j$  and  $\alpha_{k,p}$  is the attention weight from token  $k$  to position  $p$ , averaged across selected attention heads at layer depths of 0%, 50%, and 100%.

**Observation 1: Scattered pulses.** Plotting  $a_{k,j}$  over decode steps reveals that T2I attention “pulses” (brief spikes in attention to image tokens) are not well-aligned with the image being discussed. When the model’s CoT text references “Image 2,” the attention often spreads nearly uniformly across all images rather than concentrating on Image 2. We term this the *scattered pulse* phenomenon (Figure 2).

#### 3.2 Positional Attention Bias

Aggregating T2I attention across all 2,600 MuirBench samples, we examine how attention distributes across image positions.

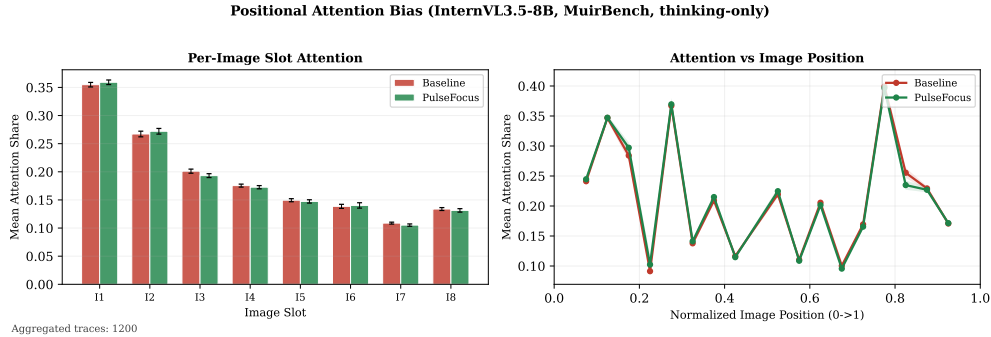


Figure 3: **Positional attention bias.** Mean T2I attention mass per image position for InternVL3.5-8B on MuirBench. Earlier images receive disproportionately more attention regardless of task. Error bars show standard deviation across task types.

**Observation 2: Earlier images receive more attention.** Figure 3 shows the mean attention mass per image position, aggregated across samples with 2–6 images. Earlier image positions (I1, I2) consistently receive higher attention than later positions, independent of task type. This positional bias mirrors findings by Fan et al. [3] but is measured here at the *internal attention level* rather than through accuracy proxies.

## 4 Method: PULSEFOCUS

Motivated by the scattered pulse and positional bias findings, we propose PULSEFOCUS, which combines structured interleaved prompting with soft attention gating at decode time. Figure 4 provides an overview of the full pipeline.

### 4.1 Interleaved Plan-Focus Prompting

Instead of free-form CoT, PULSEFOCUS constrains the output to alternate between `<plan>` and `<focus:I>` blocks:

```

PULSEFOCUS Output Format

<plan> Decide what to check. Next focus: Ix </plan>
<focus:Ix> Concrete observation about Image x... </focus>
<plan> Compare with another. Next focus: Iy </plan>
<focus:Iy> Observation about Image y... </focus>
⋮
Summary: Based on above observations...
<answer> X </answer>
```

Each `<plan>` block must end with “Next focus:  $I_x$ ” (or “END” to conclude), and each `<focus:I>` block references exactly 1 or 2 images. This structure enforces systematic image examination and prevents ad-hoc cross-image jumps.

### 4.2 Soft Attention Gating

During generation of tokens within a `<focus:Ix>` block, we apply a soft attention gate to the model’s attention computation. Let  $\mathcal{F} \subseteq \{1, \dots, N\}$  be the set of currently focused image indices. For each attention head in each decoder layer, we modify the attention logits:

$$\tilde{\alpha}_{k,p} = \alpha_{k,p} + \Delta_p, \quad \text{where} \quad \Delta_p = \begin{cases} 0 & \text{if } p \in \bigcup_{j \in \mathcal{F}} \mathcal{S}_j \\ -\lambda & \text{otherwise, if } p \in \bigcup_{j \notin \mathcal{F}} \mathcal{S}_j \end{cases} \quad (2)$$

### PulseFocus Method Overview

Decoding alternates between planning and focused observation; soft gating suppresses off-focus image tokens.

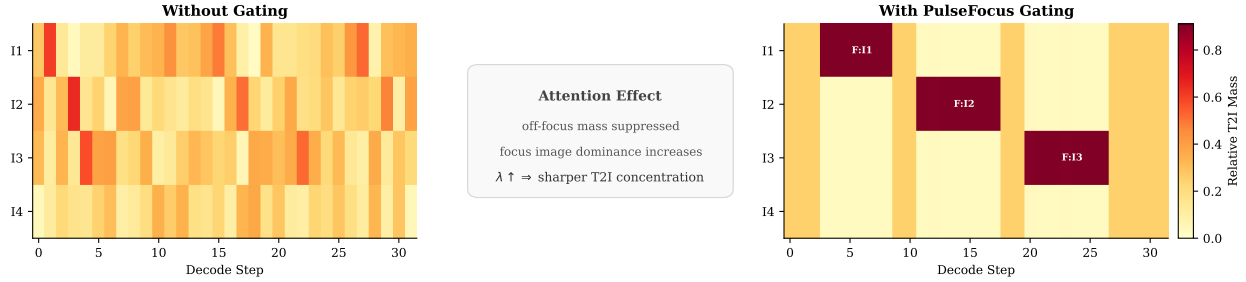
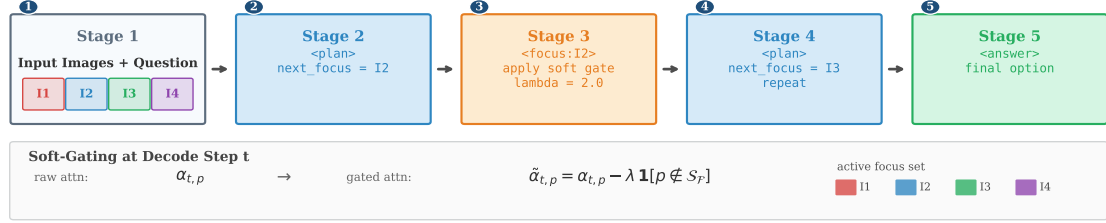


Figure 4: **PULSEFOCUS overview.** The model alternates between <plan> blocks (free attention, decides which image to examine next) and <focus:I> blocks (soft attention gate suppresses non-target images by  $-\lambda$ ). Bottom: attention heatmaps contrasting standard decoding (left, diffuse) vs. gated decoding (right, concentrated).

where  $\lambda > 0$  is the *gate strength* hyperparameter (we use  $\lambda = 2.0$ ). This soft gating reduces but does not eliminate attention to non-focused images, preserving the model’s ability to make cross-image comparisons when needed while sharpening focus on the referenced image.

During <plan> blocks, no gating is applied, allowing the model to freely attend to all images for planning.

## 4.3 Budget Control

To prevent excessive or repetitive focus cycles, we impose token budgets: each <plan> block is limited to 256 tokens, each <focus:I> block to 192 tokens, and the total number of plan-focus cycles is capped at 12. Generation terminates after the model outputs “END” in a plan block or exhausts the budget.

## 5 Experiments

### 5.1 Setup

**Datasets.** We evaluate on three multi-image benchmarks:

- **MuirBench** [14]: 2,600 test samples spanning 12+ task types including counting, scene understanding, ordering, and difference spotting. Multiple-choice format (A–D).
- **BLINK** [4]: 1,901 validation samples across 14 perceptual subtasks including jigsaw puzzles, spatial reasoning, and visual correspondence. Multiple-choice format.
- **Visual Haystacks** [16]: Needle-in-a-haystack retrieval with up to 10000 images per sample.

**Models.** We primarily experiment with the InternVL3.5 family (2B, 4B, 8B parameters) and Qwen3-VL (2B, 4B, 8B). Our main results use InternVL3.5-8B as the primary model.

Table 1: **MuirBench comparison (accuracy %)** for target model families.

Model	Params	Baseline	Ours	$\Delta$ Acc
InternVL3.5	8B	56.81	<b>57.88</b> (Gating)	+1.07
Qwen3-VL	4B	55.56	<b>56.38</b> (Budget)	+0.82

Table 2: **BLINK comparison (accuracy %)** for target model families.

Model	Params	Baseline	Ours	$\Delta$ Acc
InternVL3.5	8B	50.45	<b>54.18</b> (Budget)	+3.73
Qwen3-VL	2B	55.55	<b>56.40</b> (Budget)	+0.85

**Baselines.** We compare against: (1) **Standard CoT**: the model generates free-form chain-of-thought with standard causal attention; (2) **Cross Non-Causal**: allowing bidirectional attention across image tokens during prefill [12]; (3) **Plan-Focus (no gating)**: structured prompting without attention gating.

## 5.2 Main Results (complete results will be updated soon)

Table 1 and Table 2 present our main results. Key findings:

- **MuirBench**: among the requested target models, positive gains are observed for InternVL3.5-8B (+1.07%) and Qwen3-VL-4B (+0.82%).
- **BLINK**: PULSEFOCUS with budget control achieves **54.18%** (+3.73% over baseline 50.45%) on InternVL and +0.85% on Qwen3-VL.

## 6 Case Studies

We present qualitative examples where *per-token T2I attention colouring* reveals the failure mechanism. In each figure, every generated token is shaded by the image receiving the most attention at that decoding step. Vivid colour indicates strong focus on that image, grey or muted colour indicates diffuse, scattered attention.

### 6.1 Case 1: Counting with Scattered Attention

**MuirBench # 342** (Scene Understanding, 6 images). Question: “How many cars do you see in the given images?” Ground truth: (B) two.

Figure 1 already shows this full qualitative example (MuirBench # 342), including per-token colouring for baseline and PULSEFOCUS. To avoid duplication, we do not repeat the same figure in this section.

The critical moment is the `<focus:I5>` block. In the baseline (Figure 1), the tokens describing Image 5 are coloured with a mix of all six image colours, meaning that attention is not concentrated. The model says “one car visible on the road” for I5, then hallucinates cars in I2 (“one car visible in the distance”) and I6 (“one car parked near the building”), arriving at (C) three. With PULSEFOCUS (bottom), the `<focus:I5>` tokens are uniformly orange, indicating the soft gate ( $\lambda=2.0$ ) successfully concentrates attention on Image 5’s visual tokens. The model correctly detects “two cars visible in this image, one white and one dark-colored,” and the remaining focus blocks each report no car, yielding the correct answer (B).

### 6.2 Case 2: Image Identity Confusion

**MuirBench # 359** (Visual Retrieval, 5 images). Question: “Discover the photograph containing the same architectural edifice.” Ground truth: (B) None.

Figure 5 reveals a subtle failure: the baseline keeps returning to `<focus:I2>`, examining it three times, yet the token colouring shows dominant **red (I1)** attention throughout these blocks. The model is *talking about* Image 2 but *looking at* Image 1. This text–attention misalignment causes it to conclude “I2 matches,”

Table 3: **BLINK per-subtask results** for InternVL3.5-8B in the main setting. Accuracy (%).

Task	Baseline	PulseFocus	$\Delta$
Art Style	64.10	66.67	+2.56
Counting	63.33	64.17	+0.83
Forensic Detection	41.67	42.42	+0.76
Functional Correspondence	28.46	33.85	+5.38
IQ Test	21.33	26.67	+5.33
Jigsaw	53.33	56.67	+3.33
Multi-view Reasoning	34.59	50.38	+15.79
Object Localization	50.82	49.18	-1.64
Relative Depth	77.42	77.42	+0.00
Relative Reflectance	38.81	44.03	+5.22
Semantic Correspondence	33.09	38.85	+5.76
Spatial Relation	76.22	81.12	+4.90
Visual Correspondence	50.58	54.65	+4.07
Visual Similarity	78.52	77.04	-1.48

**Case 359: Visual retrieval identity confusion**

Q: Can you discover the photograph containing the same architectural edifice as depicted in <image>?  
 Choices: (A) <image> | (B) None of the choices provided | (C) <image> | (D) <image> | (E) <image> | GT: (B)

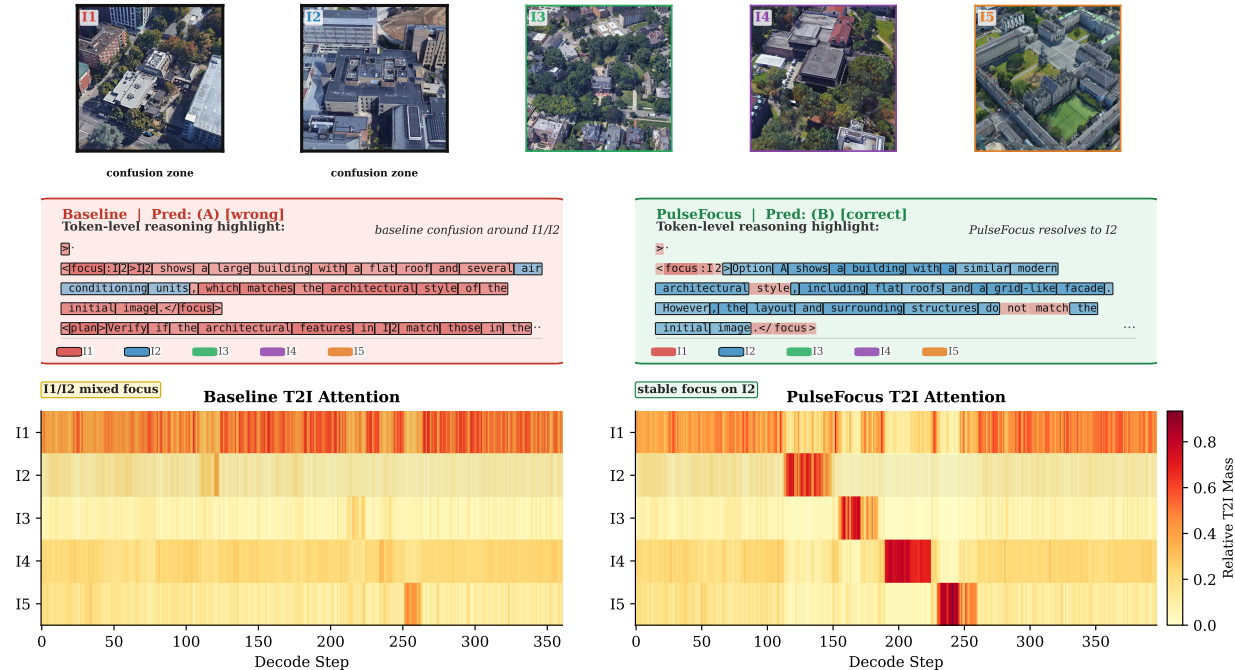


Figure 5: **Image identity confusion (MuirBench # 359, 5 images)**. **Left (Baseline)**: The model repeatedly examines “I2” but the token colours are dominantly red (I1) rather than blue (I2)—its verbal reference and actual visual attention are misaligned. It falsely concludes I2 matches the query, predicting (A). **Right (PULSEFOCUS)**: Each <focus:Ix> block’s tokens correctly match the target image’s colour, and the model concludes no match exists, predicting (B).

predicting (A). PULSEFOCUS’s gating anchors each focus block to the correct image: during <focus:I2> tokens are blue, during <focus:I3> they are green, and so on. The model correctly determines no option matches, answering (B).

## 7 Discussion

**When does PULSEFOCUS help?** The benefit is most pronounced on tasks requiring systematic comparison across images (counting, difference spotting, ordering) and on BLINK’s perceptual subtasks. On MuirBench, gains are task-dependent: tasks already well-handled by baseline CoT see smaller (or negative) gains, as the structured format adds overhead.

**Limitations.** PULSEFOCUS assumes the model can correctly parse the `<plan>/<focus:I>` format. Some models (especially smaller ones) struggle with format adherence. The gate strength  $\lambda$  is a hyperparameter that may need tuning per model. Training-based approaches (e.g., GRPO fine-tuning for the interleaved format) may unlock further gains.

## 8 Conclusion

We present an analysis of text-to-image attention dynamics in reasoning VLMs, revealing scattered attention pulses and positional bias during multi-image CoT. Our proposed PULSEFOCUS addresses these issues through structured plan-focus prompting with soft attention gating, achieving competitive results without any training. This work suggests that attention-aware inference strategies are a promising direction for improving multi-image reasoning in VLMs. As an on-going project, future work includes training models explicitly for the interleaved format via GRPO and extending evaluation to additional benchmarks.

## References

- [1] Shuai Bai, Yuxuan Cai, Ruizhe Chen, Keqin Chen, Xionghui Chen, Zesen Cheng, Lianghao Deng, Wei Ding, Chang Gao, Chunjiang Ge, et al. Qwen3-vl technical report. *arXiv preprint arXiv:2511.21631*, 2025.
- [2] Wayner Barrios and SouYoung Jin. Multi-layer learnable attention mask for multimodal tasks. *arXiv preprint arXiv:2406.02761*, 2024.
- [3] Anurag Das, Adrian Bulat, Alberto Baldrati, Ioannis Maniadis Metaxas, Bernt Schiele, Georgios Tzimiropoulos, and Brais Martinez. More images, more problems? a controlled analysis of vlm failure modes. *arXiv preprint arXiv:2601.07812*, 2026.
- [4] Xingyu Fu, Yushi Hu, Bangzheng Li, Yu Feng, Haoyu Wang, Xudong Lin, Dan Roth, Noah A Smith, Wei-Chiu Ma, and Ranjay Krishna. Blink: Multimodal large language models can see but not perceive. In *European Conference on Computer Vision*, pages 148–166. Springer, 2024.
- [5] Junqi Ge, Ziyi Chen, Jintao Lin, Jinguo Zhu, Xihui Liu, Jifeng Dai, and Xizhou Zhu. V2pe: Improving multimodal long-context capability of vision-language models with variable visual position encoding. In *Proceedings of the IEEE/CVF International Conference on Computer Vision*, pages 21070–21084, 2025.
- [6] Dongfu Jiang, Xuan He, Huaye Zeng, Cong Wei, Max Ku, Qian Liu, and Wenhui Chen. Mantis: Interleaved multi-image instruction tuning. *arXiv preprint arXiv:2405.01483*, 2024.
- [7] Bingxuan Li, Yiwei Wang, Tao Meng, Kai-Wei Chang, and Nanyun Peng. Control large language models via divide and conquer. In *Proceedings of the 2024 Conference on Empirical Methods in Natural Language Processing*, pages 15240–15256, 2024.
- [8] Bo Li, Yuanhan Zhang, Dong Guo, Renrui Zhang, Feng Li, Hao Zhang, Kaichen Zhang, Peiyuan Zhang, Yanwei Li, Ziwei Liu, et al. Llava-onevision: Easy visual task transfer. *arXiv preprint arXiv:2408.03326*, 2024.
- [9] Zhaohu Liao, Jiangtong Li, Siyu Sun, Qingyang Liu, Fengshun Xiao, Tianjiao Li, Qiang Zhang, Guang Chen, Li Niu, Changjun Jiang, et al. Divide and conquer: Exploring language-centric tree reasoning for video question-answering. In *Forty-second International Conference on Machine Learning*, 2025.

- [10] Haowei Liu, Xi Zhang, Haiyang Xu, Yaya Shi, Chaoya Jiang, Ming Yan, Ji Zhang, Fei Huang, Chunfeng Yuan, Bing Li, et al. Mibench: Evaluating multimodal large language models over multiple images. In *Proceedings of the 2024 Conference on Empirical Methods in Natural Language Processing*, pages 22417–22428, 2024.
- [11] Fanqing Meng, Jin Wang, Chuanhao Li, Quanfeng Lu, Hao Tian, Jiaqi Liao, Xizhou Zhu, Jifeng Dai, Yu Qiao, Ping Luo, et al. Mmiu: Multimodal multi-image understanding for evaluating large vision-language models. *arXiv preprint arXiv:2408.02718*, 2024.
- [12] Xiaohuan Pei, Tao Huang, YanXiang Ma, and Chang Xu. Rethinking causal mask attention for vision-language inference. *arXiv preprint arXiv:2505.18605*, 2025.
- [13] Aaditya Singh, Adam Fry, Adam Perelman, Adam Tart, Adi Ganesh, Ahmed El-Kishky, Aidan McLaughlin, Aiden Low, AJ Ostrow, Akhila Ananthram, et al. Openai gpt-5 system card. *arXiv preprint arXiv:2601.03267*, 2025.
- [14] Fei Wang, Xingyu Fu, James Y Huang, Zekun Li, Qin Liu, Xiaogeng Liu, Mingyu Derek Ma, Nan Xu, Wenxuan Zhou, Kai Zhang, et al. Muirbench: A comprehensive benchmark for robust multi-image understanding. *arXiv preprint arXiv:2406.09411*, 2024.
- [15] Wenhai Wang, Zhe Chen, Yangzhou Liu, Yue Cao, Weiyun Wang, Xizhou Zhu, Lewei Lu, Tong Lu, Yu Qiao, and Jifeng Dai. Internvl: Scaling up vision foundation models and aligning for generic visual-linguistic tasks. In *Large Vision-Language Models: Pre-training, Prompting, and Applications*, pages 23–57. Springer, 2025.
- [16] Tsung-Han Wu, Giscard Biamby, Jerome Quenum, Ritwik Gupta, Joseph E Gonzalez, Trevor Darrell, and David M Chan. Visual haystacks: A vision-centric needle-in-a-haystack benchmark. *arXiv preprint arXiv:2407.13766*, 2024.
- [17] Roy Xie, David Qiu, Deepak Gopinath, Dong Lin, Yanchao Sun, Chong Wang, Saloni Potdar, and Bhuvan Dhingra. Interleaved reasoning for large language models via reinforcement learning. *arXiv preprint arXiv:2505.19640*, 2025.
- [18] Sihan Yang, Runsen Xu, Yiman Xie, Sizhe Yang, Mo Li, Jingli Lin, Chenming Zhu, Xiaochen Chen, Haodong Duan, Xiangyu Yue, et al. Mmsi-bench: A benchmark for multi-image spatial intelligence. *arXiv preprint arXiv:2505.23764*, 2025.
- [19] Haoxuan You, Rui Sun, Zhecan Wang, Long Chen, Gengyu Wang, Hammad Ayyubi, Kai-Wei Chang, and Shih-Fu Chang. Idealgpt: Iteratively decomposing vision and language reasoning via large language models. In *Findings of the Association for Computational Linguistics: EMNLP 2023*, pages 11289–11303, 2023.
- [20] Guanghao Zhang, Tao Zhong, Yan Xia, Mushui Liu, Zhelun Yu, Haoyuan Li, Wanggui He, Fangxun Shu, Dong She, Yi Wang, et al. Cmmcot: Enhancing complex multi-image comprehension via multi-modal chain-of-thought and memory augmentation. *arXiv preprint arXiv:2503.05255*, 2025.